

# Compact vector twist sensor using a small period long period fiber grating inscribed with femtosecond laser

Fangcheng Shen (申方成)<sup>1</sup>, Xuewen Shu (舒学文)<sup>2</sup>, Kaiming Zhou (周凯明)<sup>3</sup>, Haiming Jiang (姜海明)<sup>1</sup>, Hongyan Xia (夏宏燕)<sup>1</sup>, Kang Xie (谢康)<sup>1\*</sup>, and Lin Zhang (张琳)<sup>3</sup>

<sup>1</sup>State Key Laboratory of Precision Electronic Manufacturing Technology and Equipment, School of Electromechanical Engineering, Guangdong University of Technology, Guangzhou 510006, China

<sup>2</sup>Wuhan National Laboratory for Optoelectronics & School of Optical and Electronic Information, Huazhong University of Science and Technology, Wuhan 430074, China

<sup>3</sup>Institute of Photonic and Technologies, Aston University, Birmingham B4 7ET, UK

\*Corresponding author: [kangxie@gdut.edu.cn](mailto:kangxie@gdut.edu.cn)

Received January 12, 2021 | Accepted March 4, 2021 | Posted Online July 8, 2021

We propose and demonstrate a sensitive vector twist sensor based on a small period long period fiber grating (SP-LPFG) fabricated with a femtosecond (fs) laser. The fabricated SP-LPFG is compact in size (2.8 mm) and shows strong polarization dependent peaks in its transmission spectrum due to the vectorial behavior of high-order cladding modes. Twist sensing is realized by monitoring the polarization dependent peaks, since the polarization of input light changes with fiber twist. The proposed sensor can be interrogated by the peak intensity and wavelength, with high twist sensitivity that reaches 0.257 dB/deg and 0.115 nm/deg, respectively.

**Keywords:** fiber optical sensor; long period fiber grating; twist sensor.

**DOI:** [10.3788/COL202119.090601](https://doi.org/10.3788/COL202119.090601)

## 1. Introduction

Twist (torsion) is an important parameter that reflects the stress state and health condition of structures such as bridges. Recently, the application of optical fiber sensors (OFSs) in twist sensing has intensified, due to their advantages of flexibility, light weight, and resistance to electromagnetic interference. Though many different schemes have been proposed, optical fiber twist sensors (OFTSs) can be mainly classified into two types: one interrogated with wavelength (e.g., specially designed fiber gratings<sup>[1–8]</sup>, Sagnac interferometer<sup>[9–11]</sup>, and helical fiber structure<sup>[12–14]</sup>), and the other with intensity (e.g., Solc filter<sup>[15]</sup>, Lyot filter<sup>[16]</sup>, Mach-Zehnder interferometers<sup>[17–19]</sup>, and fiber gratings<sup>[20–30]</sup>). Note that for the first type, the wavelength measurement involves the use of an expensive and bulky optical spectrum analyzer (OSA) or tunable narrow-linewidth laser, whereas, for the second type, intensity measurement only requires an optical power meter (or photodetector), which allows more compact and cost-effective interrogation than the first type. In this regard, OFTSs allowing intensity interrogation are more preferred.

The intensity-interrogated OFTSs can be further categorized into two main types: fiber interferometers and fiber gratings. The construction of fiber interferometers usually requires the use of special fiber<sup>[1–17]</sup> or modification of the fiber physical

structure<sup>[18,19]</sup>, which decreases the fiber mechanical strength, and the length of fiber interferometers can be very long (e.g., a 96 m long elliptical-core spun fiber is used in Ref. [15]). Fiber gratings can be directly introduced into the fiber without damaging the fiber physical structure, maintaining the mechanical strength and enabling more compact and stable twist sensing. To realize intensity-interrogated fiber grating twist sensors, one common principle is introducing a polarization dependent element (PDE)<sup>[20–29]</sup>. In this way, when the fiber is twisted, the input polarization entering the PDE will also change, resulting in a change of the output intensity of the PDE. Currently, fiber-grating-based PDEs mainly include a tilted fiber grating<sup>[20–26]</sup>, phase shift fiber Bragg grating (FBG)<sup>[27]</sup>, angularly cascaded long period fiber grating (LPFG)<sup>[28]</sup>, and grating in special fiber, such as polarization maintaining fiber<sup>[29]</sup>.

Recently, we found that polarization dependent coupling can be achieved in LPFGs with much smaller grating periods, i.e., the so-called small period LPFG (SP-LPFG)<sup>[31]</sup>. Thanks to the strong polarization dependence, SP-LPFGs are good candidates for the PDE in twist sensing applications. In this work, we propose and demonstrate a sensitive OFTS based on an SP-LPFG that is inscribed with a femtosecond (fs) laser in a normal single mode fiber (SMF). The adopted SP-LPFG is compact in size with a total length of only 2.8 mm and is insensitive to strain and temperature change. Apart from intensity-based interrogation, the

proposed sensor also exhibits sensitive wavelength shift to twist and thus can be interrogated by wavelength.

## 2. Principle and Fabrication

As shown schematically in Fig. 1, LPFG is a kind of all in fiber device that consists of periodic modification along the fiber axis (usually the modification of the refractive index). In LPFGs, light of the core mode is coupled to fiber cladding modes, which attenuates quickly, leaving serial attenuation peaks in the transmission spectrum of the LPFG. The wavelengths of those attenuation peaks can be determined from the phase matching condition:

$$\lambda_{\text{peak}} = (n_{\text{eff-co}} - n_{\text{eff-cl}}^i) \cdot \Lambda, \quad (1)$$

where  $n_{\text{eff-co}}$  and  $n_{\text{eff-cl}}^i$  are the effective indexes of the core mode and cladding mode, with  $i$  denoting the cladding mode order, and  $\Lambda$  is the grating period. Standard LPFGs usually have a period of several hundred micrometers, and core mode light is coupled to low-order cladding modes that satisfy the weakly guiding approximation, whereas in SP-LPFGs, with a small grating period less than 50  $\mu\text{m}$ , coupling to high-order cladding modes is enabled. These high-order cladding modes are far away from weakly guiding regime and present strong vectorial behavior<sup>[32–34]</sup>, resulting in the strong polarization dependent peaks in SP-LPFGs. Such strong polarization dependence makes SP-LPFGs good candidates for the PDE in twist sensing applications.

In our experiment, a fs laser (800 nm, 1 kHz, 150 fs) was focused into the core of a stripped SMF (SM 28) by a 100 $\times$  objective lens. The stripped SMF was mounted on a high resolution three-dimensional stage to gain translational motion relative to the laser focus. To keep the fiber straight, constant axial stress is applied to the fiber. The fiber position was monitored by a CCD camera, guaranteeing that the fiber is at the right position. The whole fabrication process was controlled by a computer. To fabricate the LPFG, a pulse energy of 200 nJ was used, and the fiber was translated along the fiber axis with a constant speed of 20  $\mu\text{m/s}$ ; at the same time, the laser was turned on and off periodically by a mechanical shutter to introduce the periodic refractive index modulations (RIMs) into the fiber core, which construct the grating. During the fabrication, the transmission spectrum of the LPFG was monitored by an OSA in real time.

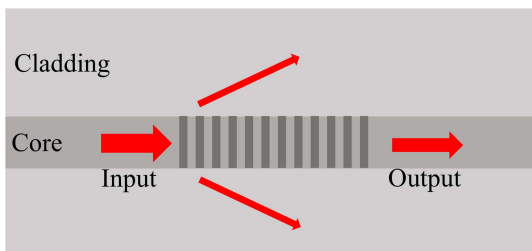


Fig. 1. Schematic of long period fiber grating.

Figure 2 depicts the experimentally measured transmission spectrum of the fabricated grating, which has a period of 40  $\mu\text{m}$  and a duty cycle of 50%, and 70 periods are introduced, corresponding to a total length of 2.8 mm (see inset of Fig. 2). This length is much more compact than that of normal LPFGs (usually tens of millimeters), since the induced RIM is highly localized in the core, i.e., occupying part of the fiber core in the cross section. Compared with the RIM that occupies the whole core transversely in normal LPFGs (Fig. 1), such highly localized RIM suppresses the cancellation of negative and positive coupling to high-order cladding modes, thus allowing much stronger coupling. The spectrum in Fig. 2 is measured with un-polarized light, where the deepest dip shows strength of  $\sim 15$  dB. The insertion loss is  $\sim 4$  dB (indicated by the red dash line in Fig. 2), which mainly results from Mie scattering of the localized RIM<sup>[35]</sup>. The insertion loss can be reduced by using decreased laser energy, at a cost of lower coupling efficiency, which should be balanced according to the requirements of practical applications. Note that though a relatively higher pulse energy is used, the grating survives at  $> 3000 \mu\epsilon$  strain, which is comparable to LPFGs inscribed with a  $\text{CO}_2$  laser<sup>[36]</sup>, indicating that the mechanical strength of the grating is well maintained.

To realize polarization-related twist sensing, more of our concern is the polarization dependence. During the measurement, the polarization of light entering the grating is controlled by a polarizer followed by a polarization controller (PC), and the measured spectra of the peak around 1528 nm for two orthogonal polarizations are shown in Fig. 3. It can be seen from Fig. 3 that two peaks are fully distinguishable with polarized input light, and a strength over 25 dB is achieved for one of the polarizations (blue line in Fig. 3). Such strong polarization dependence mainly results from the vectorial nature of the high-order cladding modes, since the grating period is very small<sup>[31]</sup>. Sensitive twist sensing will be achieved by the strong polarization dependence, as will be discussed in the next section.

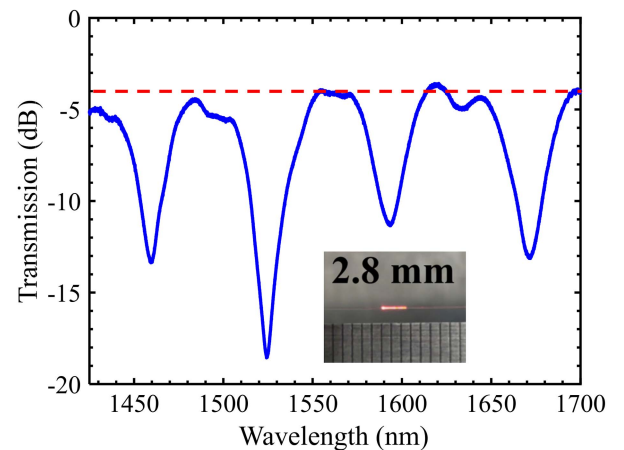


Fig. 2. Transmission spectrum of the fabricated grating measured with un-polarized light. Inset shows the photograph of the grating, where the grating length is indicated by the red light scattered out of the fiber, and the interval of the ruler is millimeters [mm].

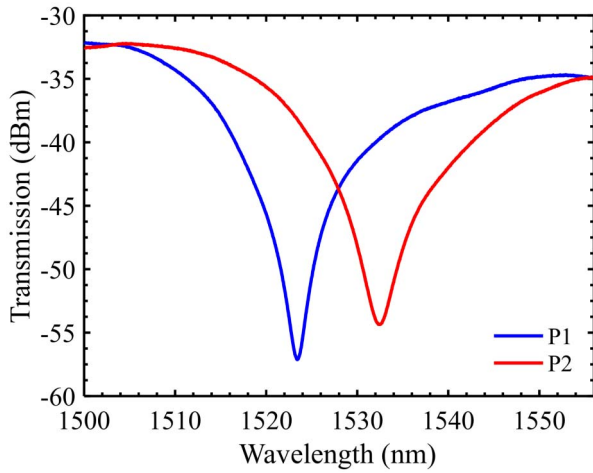


Fig. 3. Transmission spectra of the fabricated grating with two orthogonal input polarizations (P1 and P2).

### 3. Experiment and Discussion

The schematic of the setup for twist sensing is depicted in Fig. 4, broadband light from a super-continuum (SC) source passes

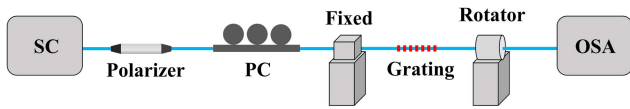


Fig. 4. Schematic of the experimental setup for twist sensing. SC, super-continuum source; PC, polarization controller.

through a polarizer, providing the initial polarized light whose polarization is controlled by the following PC, and the evolution of the output spectrum is monitored with an OSA. The grating is fixed between a fiber holder and a fiber rotator with an engraved dial. During the measurement, the grating is slightly strained to keep it straight, thus eliminating the unwanted perturbation such as bending.

Before rotating the fiber, we adjusted the initial polarization state using the PC to fully excite the peak on the shorter wavelength side (represented by P1 in Fig. 3). To characterize the twist sensing properties of the grating, the fiber rotator was rotated by 180 deg clockwise with 10 deg steps, and the transmission spectrum was recorded every 10 deg. Figure 5(a) shows the spectral evolution of the grating under twist. It can be clearly seen that, with the increase of twist angle, the strength of the peak on the short wavelength side decreases [see black circles in Fig. 5(a)], and beyond certain angles, this peak fully disappears, whereas the other peak appears and starts to grow. The dependence of the peak intensity on twist angle is depicted in Fig. 5(b), which shows a sine-like function that agrees with previous reports<sup>[24]</sup>. The slopes of two linear fitting regions from 0 to 40 deg and from 130 to 170 deg are 0.257 dB/deg and  $-0.131$  dB/deg, respectively. In view of the practical application, the grating can be pre-twisted to this region in order to achieve a high sensitivity and linear response. The twist direction can also be detected with the pre-twist, depending on whether the peak intensity increases or decreases. It should be noted that the peak intensity is not a monotonic function of twist angle, i.e., different twist angles can result in the same peak

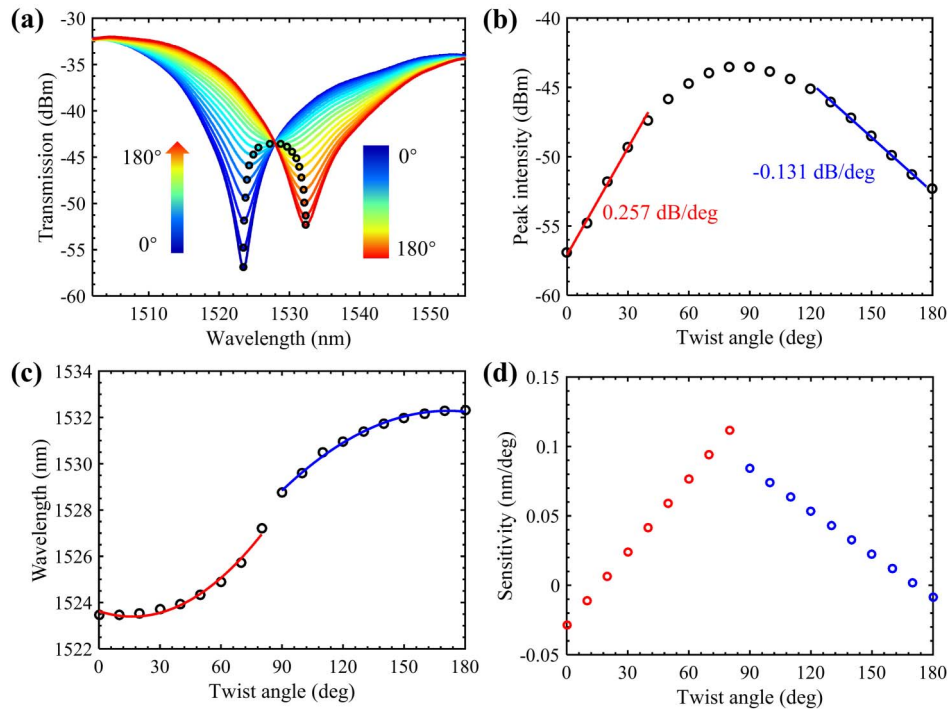


Fig. 5. Evolution of (a) transmission spectra [peak positions are denoted by black circles], (b) peak intensity, (c) peak wavelengths with increasing twist angle, and (d) wavelength-interrogated twist sensitivity calculated from the fitted function at each measurement point.

**Table 1.** Sensing Performance of Fiber-Grating-Based Twist Sensors.

Interrogation	Method	Sensitivity	Length (mm)	Orientation	Reference (year)
Intensity	SP-LPFG	0.257 dB/deg	2.8	Vector	This work
	Cascaded LPFGs	-0.268 dB/deg	47.56	Scalar	[28] (2018)
	ITO-coated TFBG	0.274 dB/deg	15	Vector	[21] (2020)
	SMF-TFBG	0.299 dB/deg	10	Scalar	[23] (2014)
	MMF-TFBG	0.075 dB/deg	NA	Vector	[22] (2014)
	Phase shift FBG	0.088 dB/deg	1.72	Vector	[27] (2016)
	Cascaded HLPFG	0.0074 dB/deg	58	Vector	[30] (2014)
Wavelength	SP-LPFG	0.115 nm/deg	2.8	Vector	This work
	CO <sub>2</sub> LPFG	0.019 nm/deg	20	Vector	[2] (2004)
	HLPFG	0.067 nm/deg	34	Vector	[5] (2017)
	Improved HLPFG	0.029–0.11 nm/deg	18–36	Vector	[37] (2020)

intensity. Therefore, to guarantee reliable twist sensing, the detectable angle range using peak intensity should be limited to 90°, or supplementary judgment by wavelength [Fig. 5(c)] is required.

It can be seen from Fig. 5(a) that the peak wavelength [denoted by black circle in Fig. 5(a)] also evolves with twist angle, suggesting that the grating can also work as a wavelength-interrogated twist sensor. Figure 5(c) depicts the peak wavelength as a function of the twist angle, where the wavelength evolution of the deepest peaks is fitted with quadratic functions separately [see blue and red lines in Fig. 5(c)]. Figure 5(d) shows the sensitivity calculated from the fitted function in Fig. 5(c) at each measurement point, with a maximum sensitivity of ~0.115 nm/deg.

A comparison between our work and several typical previously reported OFTSs based on the fiber grating is listed in Table 1, including tilted FBG (TFBG) both in SMF and multi-mode fiber (MMF), and helical LPFG (HLPFG), where the unit of the twist sensitivity is unified for convenient comparison. It can be seen from Table 1 that our SP-LPFG sensor offers high sensitivity as well as compactness and vector sensing ability, while requiring no additional coating or use of a special fiber. Moreover, the measured wavelength sensitivity in Fig. 5 is higher than many of the reported schemes (see wavelength-interrogated schemes in Table 1), indicating the potential of the SP-LPFG in wavelength-interrogated twist sensing application.

The cross sensitivity of the proposed twist sensor to strain is also characterized, utilizing the setup depicted in Fig. 4. To investigate the influence of strain on twist sensing, the spectral response of the grating to strain is measured with pre-twist angles of 10, 30, and 50 deg, respectively. Figure 6 depicts the measured evolution of peak intensity and wavelength with increasing strain, where the linear fitting for each measurement

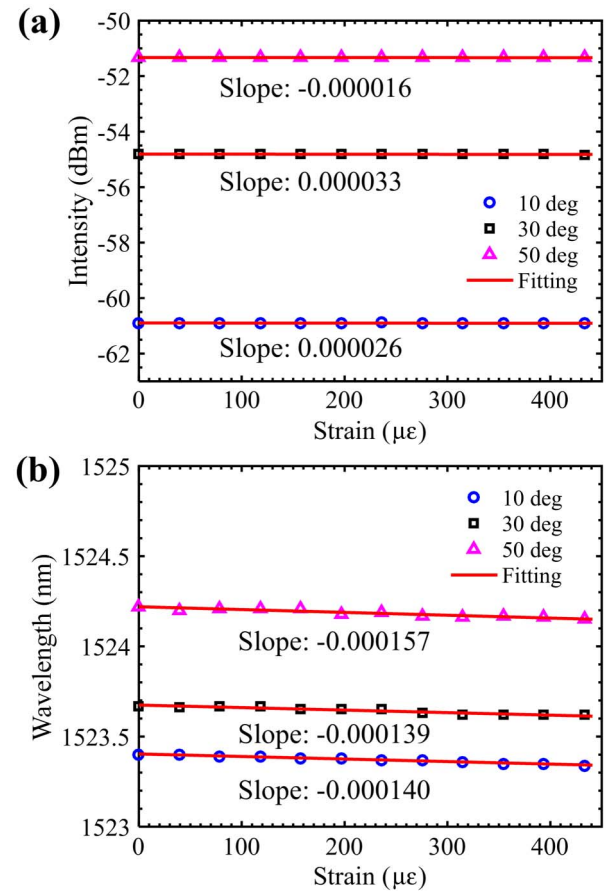


**Fig. 6.** Evolution of (a) peak intensity and (b) peak wavelength with increased strain, when the grating was pre-twisted with an angle of 10 deg [blue circles], 30 deg [black rectangles], and 50 deg [magenta triangles]. The linear fitting of the evolution is depicted by red lines.



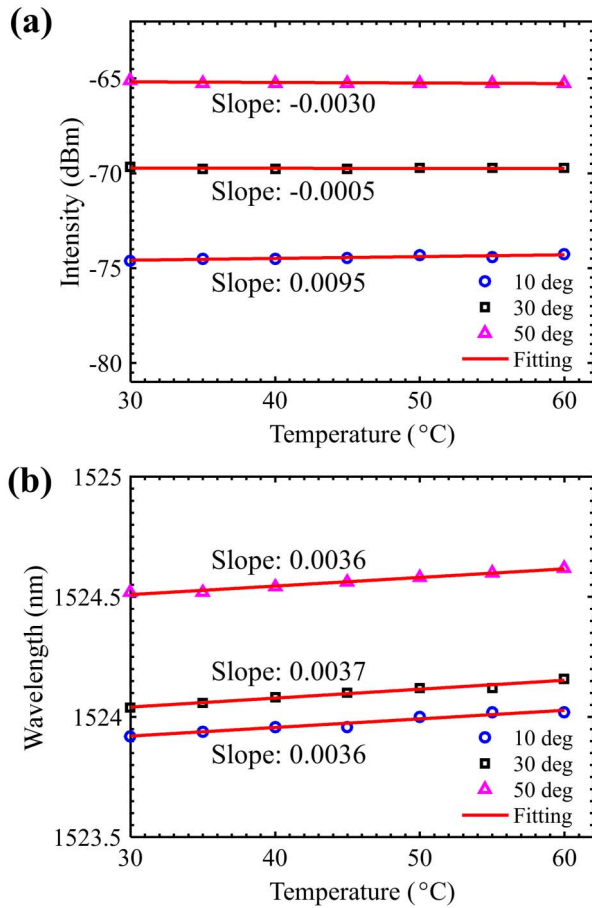


**Fig. 7.** Evolution of (a) peak intensity and (b) peak wavelength with increased temperature, when the grating was pre-twisted with an angle of 10 deg (blue circles), 30 deg (black rectangles), and 50 deg (magenta triangles). The linear fitting of the evolution is depicted by red lines.

is also shown (see the red lines in Fig. 6). We can see that the slope of each fitting is very small, with a maximal slope of  $0.000033 \text{ dB}/\mu\epsilon$  for peak intensity and  $-0.000157 \text{ nm}/\mu\epsilon$  for peak wavelength, suggesting that the proposed twist sensor is insensitive to strain, which is one of the important perturbations in twist measurement.

We also characterized the cross sensitivity of the proposed grating to temperature, which is another important perturbation in twist measurement. During the characterization, the grating was heated from  $30^\circ\text{C}$  to  $60^\circ\text{C}$  with  $5^\circ\text{C}$  steps, under pre-twist angles of 10, 30, and 50 deg, respectively. The measured results are depicted in Fig. 7, with the maximal coefficient of  $0.0095 \text{ dB}/^\circ\text{C}$  for intensity interrogation [Fig. 7(a)] and  $0.0037 \text{ nm}/^\circ\text{C}$  for wavelength interrogation [Fig. 7(b)], respectively, indicating a low temperature cross sensitivity.

#### 4. Conclusion

To conclude, a sensitive vector twist sensor based on SP-LPFG is proposed and demonstrated. The SP-LPFG is much more

compact compared with normal LPFGs, with a total length of only 2.8 mm. The proposed twist sensor can be interrogated by both intensity and wavelength, and high twist sensitivity of  $0.257 \text{ dB}/\text{deg}$  and  $0.115 \text{ nm}/\text{deg}$  is achieved for the two interrogation schemes. Such high sensitivity is achieved without modifying the physical structure of the fiber, such as post-coating or partially removing the fiber cladding, enabling more stable grating structures. Moreover, the proposed sensor is insensitive to strain and temperature, which are two of the most important perturbations in twist measurement. With the above advantages, the proposed sensor is a good candidate for structure monitoring applications.

#### Acknowledgement

This work was supported by the National Natural Science Foundation of China (Nos. 11574070, 11874126, and 51803037), the Leading Talents of Guangdong Province Program (No. 2016LJ06D506), and the Natural Science Foundation of Guangdong Province, China (No. 2019A1515011229).

#### References

1. C. Sun, R. Wang, X. Jin, Z. Wang, W. Liu, S. Zhang, Y. Ma, J. Lin, Y. Li, T. Geng, W. Sun, Z. Qu, and L. Yuan, "A new phase-shifted long-period fiber grating for simultaneous measurement of torsion and temperature," *Chin. Opt. Lett.* **18**, 021203 (2020).
2. Y. Wang and Y. Rao, "Long period fibre grating torsion sensor measuring twist rate and determining twist direction simultaneously," *Electron. Lett.* **40**, 164 (2004).
3. Y. Li, L. Chen, Y. Zhang, W. Zhang, S. Wang, Y. Zhang, T. Yan, W. Hu, X. Li, and P. Geng, "Realizing torsion detection using Berry phase in an angle-chirped long-period fiber grating," *Opt. Express* **25**, 13448 (2017).
4. Y. Zhang, W. Zhang, P. Wu, L. Bie, L. Kong, Z. Li, Y. Zhang, and T. Yan, "Torsion bidirectional sensor based on tilted-arc long-period fiber grating," *Opt. Express* **27**, 37695 (2019).
5. X. Kong, K. Ren, L. Ren, J. Liang, and H. Ju, "Chiral long-period gratings: fabrication, highly sensitive torsion sensing, and tunable single-band filtering," *Appl. Opt.* **56**, 4702 (2017).
6. R. Subramanian, C. Zhu, H. Zhao, and H. Li, "Torsion, strain, and temperature sensor based on helical long-period fiber gratings," *IEEE Photon. Technol. Lett.* **30**, 327 (2017).
7. M. Deng, J. Xu, Z. Zhang, Z. Bai, S. Liu, Y. Wang, Y. Zhang, C. Liao, W. Jin, G. Peng, and Y. Wang, "Long period fiber grating based on periodically screw-type distortions for twist sensing," *Opt. Express* **25**, 14308 (2017).
8. C. Jiang, Y. Liu, L. Huang, and C. Mou, "Double cladding fiber chiral long-period grating-based directional torsion sensor," *IEEE Photon. Technol. Lett.* **31**, 1522 (2019).
9. O. Frazão, R. M. Silva, J. Kobelke, and K. Schuster, "Temperature and strain-independent torsion sensor using a fiber loop mirror based on suspended twin-core fiber," *Opt. Lett.* **35**, 2777 (2010).
10. L. Htein, D. S. Gunawardena, Z. Liu, and H. Tam, "Two semicircular-hole fiber in a Sagnac loop for simultaneous discrimination of torsion, strain and temperature," *Opt. Express* **28**, 33841 (2020).
11. B. Song, H. Zhang, Y. Miao, W. Lin, J. Wu, H. Liu, D. Yan, and B. Liu, "Highly sensitive twist sensor employing Sagnac interferometer based on PM-elliptical core fibers," *Opt. Express* **23**, 15372 (2015).
12. H. Zhang, Z. Wu, P. P. Shum, X. Shao, R. Wang, X. Q. Dinh, S. Fu, W. Tong, and M. Tang, "Directional torsion and temperature discrimination based on a multicore fiber with a helical structure," *Opt. Express* **26**, 544 (2018).

13. F. Zhang, Y. Wang, Z. Bai, S. Liu, C. Fu, Y. Huang, C. Liao, and Y. Wang, "Helicity enhanced torsion sensor based on liquid filled twisted photonic crystal fibers," *Sensors* **20**, 1490 (2020).
14. Y. Li, P. Lu, Z. Qu, W. Zhang, W. Ni, D. Liu, and J. Zhang, "An optical fiber twist sensor with temperature compensation mechanism based on T-SMS structure," *IEEE Photon. J.* **12**, 6800308 (2019).
15. C. Sun, M. Wang, and S. Jian, "Experimental and theoretical study of the in-fiber twist sensor based on quasi-fan Solc structure filter," *Opt. Express* **25**, 19955 (2017).
16. B. Huang, X. Shu, and Y. Du, "Intensity modulated torsion sensor based on optical fiber reflective Lyot filter," *Opt. Express* **25**, 5081 (2017).
17. Y. Ren, X. Liu, X. Zhang, and J. Yang, "Two-mode fiber based directional torsion sensor with intensity modulation and 0° turning point," *Opt. Express* **27**, 29340 (2019).
18. Q. Fu, J. Zhang, C. Liang, I. P. Ikehukwu, G. Yin, L. Lu, Y. Shao, L. Liu, D. Liu, and T. Zhu, "Intensity-modulated directional torsion sensor based on in-line optical fiber Mach-Zehnder interferometer," *Opt. Lett.* **43**, 2414 (2018).
19. Z. Bai, M. Deng, S. Liu, Z. Zhang, J. Xu, J. Tang, Y. Wang, C. Liao, and Y. Wang, "Torsion sensor with rotation direction discrimination based on a pre-twisted in-fiber Mach-Zehnder interferometer," *IEEE Photon. J.* **9**, 7103708 (2017).
20. C. Shen, Y. Zhang, W. Zhou, and J. Albert, "Au-coated tilted fiber Bragg grating twist sensor based on surface plasmon resonance," *Appl. Phys. Lett.* **104**, 071106 (2014).
21. R. Wang, Z. Li, X. Chen, N. Hu, Y. Xiao, K. Li, and T. Guo, "Mode splitting in ITO-nanocoated tilted fiber Bragg gratings for vector twist measurement," *J. Lightwave Technol.* **39**, 4151 (2021).
22. T. Guo, F. Liu, B. O. Guan, and J. Albert, "Polarimetric multi-mode tilted fiber grating sensors," *Opt. Express* **22**, 7330 (2014).
23. Y. Lu, C. Shen, D. Chen, J. Chu, Q. Wang, and X. Dong, "Highly sensitive twist sensor based on tilted fiber Bragg grating of polarization-dependent properties," *Opt. Fiber Technol.* **20**, 491 (2014).
24. X. Chen, K. Zhou, L. Zhang, and I. Bennion, "In-fiber twist sensor based on a fiber Bragg grating with 81° tilted structure," *IEEE Photon. Technol. Lett.* **18**, 2596 (2006).
25. K. Yang, Y. Liu, Z. Wang, Y. Li, Y. Han, and H. Zhang, "Twist sensor based on long period grating and tilted Bragg grating written in few-mode fibers," *IEEE Photon. J.* **10**, 7102708 (2018).
26. X. Guo, Z. Xing, H. Qin, Q. Sun, H. Wang, D. Liu, L. Zhang, and Z. Yan, "Low-cost temperature- and strain-insensitive twist sensor based on a hybrid fiber grating structure," *Appl. Opt.* **58**, 4479 (2019).
27. B. Huang and X. Shu, "Ultra-compact strain and temperature-insensitive torsion sensor based on a line-by-line inscribed phase-shifted FBG," *Opt. Express* **24**, 17670 (2016).
28. J. Yang, W. Zhang, Y. Zhang, X. Kang, Y. Zhang, L. Kong, T. Yan, and L. Chen, "Temperature-insensitive polarimetric torsion sensor based on a pair of angularly cascaded LPFGs," *Opt. Fiber Technol.* **46**, 11 (2018).
29. D. K. Kim, J. Kim, S. L. Lee, S. Choi, M. S. Kim, and Y. W. Lee, "Twist-direction-discriminable torsion sensor using long-period fiber grating inscribed on polarization-maintaining photonic crystal fiber," *IEEE Sens. J.* **20**, 2953 (2019).
30. L. Xian, P. Wang, and H. Li, "Power-interrogated and simultaneous measurement of temperature and torsion using paired helical long-period fiber gratings with opposite helicities," *Opt. Express* **22**, 20260 (2014).
31. F. Shen, C. Wang, Z. Sun, K. Zhou, L. Zhang, and X. Shu, "Small-period long-period fiber grating with improved refractive index sensitivity and dual-parameter sensing ability," *Opt. Lett.* **42**, 199 (2017).
32. Y. Sun, Z. Yan, K. Zhou, B. Luo, B. Jiang, C. Mou, Q. Sun, and L. Zhang, "Excessively tilted fiber grating sensors," *J. Lightwave Technol.* **39**, 3761 (2021).
33. M. Z. Alam and J. Albert, "Selective excitation of radially and azimuthally polarized optical fiber cladding modes," *J. Lightwave Technol.* **31**, 3167 (2013).
34. F. Shen, K. Zhou, C. Wang, H. Jiang, D. Peng, H. Xia, K. Xie, and L. Zhang, "Polarization dependent cladding modes coupling and spectral analyses of excessively tilted fiber grating," *Opt. Express* **28**, 1076 (2020).
35. M. L. Åslund, N. Nemanja, N. Groothoff, J. Canning, G. D. Marshall, S. D. Jackson, A. Fuerbach, and M. J. Withford, "Optical loss mechanisms in femtosecond laser-written point-by-point fibre Bragg gratings," *Opt. Express* **16**, 14248 (2008).
36. G. Chen, H. Xiao, Y. Huang, Z. Zhou, and Y. Zhang, "A novel long-period fiber grating sensor for large strain measurement," *Proc. SPIE* **7292**, 729212 (2009).
37. Y. Zhao, S. Liu, J. Luo, Y. Chen, C. Fu, C. Xiong, Y. Wang, S. Jing, Z. Bai, C. Liao, and Y. Wang, "Torsion, refractive index, and temperature sensors based on an improved helical long period fiber grating," *J. Lightwave Technol.* **38**, 2504 (2020).